

A stable and low loss oxide for superconducting qubits

Zengqian Ding^{1,a)}, Boyi Zhou^{1,a)}, Tao Wang^{1,a)}, Lina Yang¹, Yanfu Wu¹, Xiao Cai¹,

Kanglin Xiong^{1,2,b)}, Jiagui Feng^{1,2,c)}

¹ Gusu Laboratory of materials, Suzhou, 215123

² Suzhou Institute of Nano-Tech and Nano-Bionics, CAS, Suzhou, 215123

^{a)} Zengqian Ding, Boyi Zhou, and Tao Wang contributed equally to this work

^{b)} E-mail: klxiong2008@sinano.ac.cn

^{c)} E-mail: jgfeng2017@sinano.ac.cn

Abstract: The dielectric loss of amorphous oxide layers is a major limiting factor for the coherent time of superconducting qubits. Usually, the surface oxides of superconductor film are lossy and unstable in air. To increase the coherence time, it is essential for qubits to have stable and low dielectric loss oxides, either as barrier or passivation layers. Here, we demonstrate that a kind of amorphous tantalum oxide on Ta film is robust and stable by means of chemical and structural analysis. Such kind of oxide layer forms in a self-limiting process on the surface of α -Ta (110) film in piranha solution, yielding stable thickness and steady chemical composition. Quarter-wavelength coplanar waveguide resonators are made to study the loss of this oxide. An internal quality factor of above three million is measured at single photon level for fresh device, and it is still over two million even after exposed to air for months. Furthermore, we propose a method to fabricate all-tantalum superconducting qubits using this kind

of oxide as the dielectric and passivation layers.

1. Introduction

Superconducting quantum computing has gained substantial experimental progresses over the last two decades. It is now one of the leading candidates to build a fault-tolerant quantum computer[1]. F. Arute et al. achieved quantum “supremacy” in 2019 with a chip of 53 Xmon qubits[2]. To demonstrate real quantum advantage, the quality and quantity of qubits need to increase simultaneously. In recent years, the coherence time (T_1) of Transmon qubits on plane surface has increased to hundreds of microseconds due to the improvement of material quality and fabrication methods[3-6]. In 2020, A. P. M. Place et al. reported coherence time of exceeding 0.3ms for the Transmon fabricated with alpha-phase tantalum films [7]. Following this report, C. Wang et al. increased the coherence time to 0.5ms in 2021[8].

It is believed that most lossy channels emerged in the material growth and device fabrication[9, 10]. Specifically, the dielectric loss arises from three interfaces[11], i.e., the amorphous oxide layer at the superconductor-air (MA) interface, the amorphous oxide layer at the substrate-air (SA) interface, and the amorphous layer at the superconductor-substrate (MS) interface. The MS interface can be improved by substrate cleaning, epitaxial film growth, and subsequently etching method for the qubit fabrication[12-15]. However, the amorphous oxide layers in the MA interface is inherent with material properties and hard to manage. Most superconductors used in the qubits are metals which are easy to oxidize in air, and the thicknesses of these oxides increase over time. Constant efforts have been paid to reduce loss of the MA interface.

Verjauw et al. discovered that removing the niobium (Nb) oxides can increase the internal quality factor(Q_i) with half magnitude[16]. Other groups also found that passivation of the superconductor surface can improve the quality of the devices[17]. Besides the three interfaces, the Josephson junction can also be lossy and noisy. The best insulator layer in the Josephson junction is still amorphous alumina, which is unstable and has large dielectric loss.

In this paper, we investigate the surface oxide of α -Ta (110) films prepared in piranha and study its effects on the Q_i of the coplanar waveguide (CPW). Combining the chemical and structural analysis, we find that the oxide is a dense layer of amorphous Ta_2O_5 whose thickness and chemical composition are stable in air and piranha. CPW resonators are made of α -Ta (110) film with such surface oxide. The Q_i is three million in the single-photon regime at 10 mK for fresh device, and is above two million for device exposed to the atmosphere for months. The high Q_i and robustness of the resonators indicate that such Ta_2O_5 layer is of low dielectric loss and stable. Thus, we propose a method to fabricate all-tantalum superconducting qubits with such oxide as dielectric barrier and passivation layers.

2. Experiment

The Ta films with thickness of 200 nm were deposited on 2-inch sapphire substrates by DC magnetron sputtering in a high vacuum chamber. The film shows the crystallographic plane of α -Ta (110) confirmed by X-ray Diffraction (XRD). For

comparison, four different samples from the same wafer were prepared, i.e., a fresh one, two soaked in fresh piranha for 1 and 3 times and 20 minutes each time, and one exposed to air for 4 months. Surface morphology and roughness are measured by atomic force microscopy (AFM). The thicknesses and chemical compositions of oxide layers are investigated using scanning transmission electron microscope (TEM/STEM) and angle-resolved X-ray photoelectron spectroscopy (XPS). For the XPS, the spot size is 250 μm , and the angle varies from 0 to 75 degrees which is defined as the angle between the normal direction of the wafer surface and the direction of the signal acceptance. Q_i of the Ta CPW resonators are measured at 10 mK with power down to single photon level in a dilution refrigerator with magnetic shield and infrared filters.

3. Results and discussion

The surface of as grown α -Ta (110) film with optimal deposition condition is shown in Fig. 1(a). The grains of Ta are elongated and tightly packed given a surface roughness (R_q) of 1.09nm in the area of $2 \mu\text{m} \times 2 \mu\text{m}$. After exposed to air for hours, the film surface is covered with an amorphous oxide layer uniformly, with no sign of further oxidation of grain boundary under TEM. The thickness of this layer is 2.24nm [Fig. 1(d)], which increases to 2.41nm after leaving the film in air for another four months. Conversely, with immersion in piranha solution for one time, the thickness of the amorphous oxide layers increases to 2.61nm and the surface still remains alike [Fig. 1(b) and (e)]. Then exposing the sample to air and immersing the sample in piranha

solution again for more time, there is no noticeable change of its surface and thickness [Fig. 1(c) and (f)]. The results suggest that the oxidization of the α -Ta (110) surface in air and piranha are self-limiting processes which probably evolve logarithmically with time [18, 19]. The difference is that, in air, the surface oxide layer grows slowly and takes longer time to saturate; but in the piranha, which is a strong oxidizer, the surface oxide layer reaches its limited thickness in a shorter time.

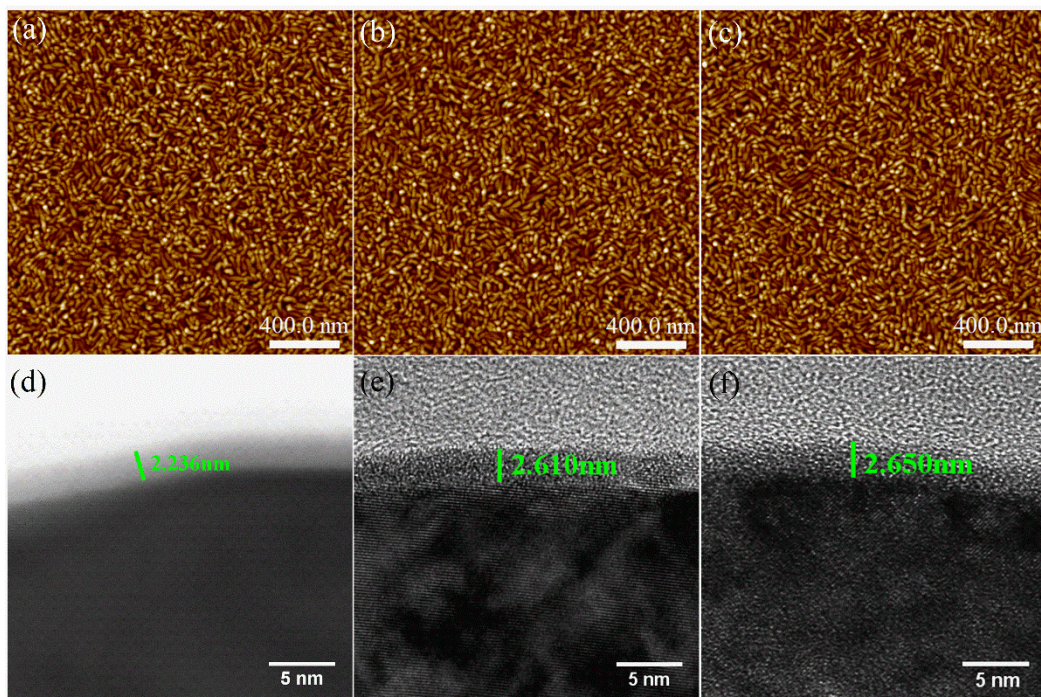


Fig. 1. AFM images of Ta films measured over a $2\mu\text{m}\times 2\mu\text{m}$ area, and TEM/STEM images of Ta film surface oxide layer. (a) - (c) Ta film images before immersion in piranha solution and immersion in piranha solution once, 3 times, respectively. (d) the oxide layer thickness of the fresh Ta film. (e) (f) the oxide layer thickness after immersion in piranha solution once, and 3 times, respectively.

Besides the structure characterization, the chemical composition of the surface oxide layer is measured by the XPS. Fig. 2(a) shows the XPS data obtained at angle of

0° for two samples with oxides grown in air and piranha, respectively. Compared with the oxide grown in piranha solution (Blue curve), the oxide grown in air (Orange curve) has an obvious shoulder on the right of the two peaks at lower binding energy which are correspond to the orbitals of sub-oxides. This is further confirmed by the angle-resolved testing as shown in Fig. 2(b). The oxide layer of Ta film immersed in piranha solution contains only Ta⁵⁺ from surface to subsurface. However, with the detecting depth increasing, the oxide layer of Ta film exposed to air start to contain multiple valence states. These states can be fitted with the oxidization valance of Ta³⁺ and Ta²⁺. Considering the factor that the oxide prepared in piranha is pure Ta₂O₅ in a dense amorphous structure, no wonder it is very stable in air and in piranha solution. From the angle-resolved data[20], the thicknesses of the surface oxide layer are also obtained. They are 2.45 nm for the one exposed to the air and 2.74 nm for the one immersed in piranha solution, which is consistent with the TEM data, with deviation of about 0.2 nm. The agreement of thicknesses measured by two distinct methods suggest again that the surface oxide on α-Ta (110) film formed in piranha solution is uniform.

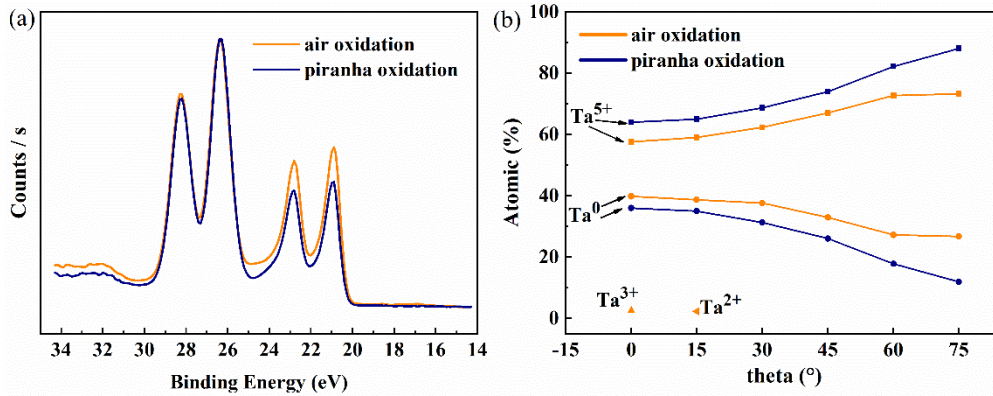


Fig. 2. Angle-resolved XPS spectra ($\theta=0^\circ$, the θ is the angle between the normal of the film surface and the signal acceptance angle) of Ta film and Ta chemical elements atomic ratio in the oxide layer. (a) The spectra of Ta film exposed to atmosphere (Orange curve) and immersed in piranha solution (Blue curve), respectively. The two peaks at low binding energy belong to $4f_{7/2}$ and $4f_{5/2}$ orbitals of Ta metal, and the two peaks at higher binding energy correspond to the same orbitals of Ta_2O_5 . (b) Surface chemical elements atomic ratio according to angle-resolved XPS spectra in the oxide layer of Ta film exposed to atmosphere (Orange curve) and immersed in piranha solution (Blue curve), respectively.

As to the superconducting device, the metallic and semiconductor nature of sub-oxides lead to conductivity losses[5]. Thus the amorphous Ta_2O_5 layer is a preferred choice for low loss devices. Since the losses as a whole can be estimated from Qi of resonators, we fabricate CPW resonators using the α -Ta (110) film covered with such oxides. To begin with, the sapphire wafer with α -Ta (110) film was soaked in piranha. The resonators were defined with optical lithography and a wet etching process. Then, the wafer was cut into $8\text{ mm} \times 8\text{ mm}$ square chips. Last, the chips were rinsed in piranha

again.

The Q_i of a fresh resonator and a resonator that had been exposed to air for four months are measured and shown in Fig. 3. The fresh resonator has a Q_i of 3.0×10^6 in the single photon region. It is higher than that (2.0×10^6) of the fresh resonator made from an aluminum (Al) film deposited by molecular beam epitaxy on sapphire substrate[13]. And it is also higher than that (1.0×10^6) of the fresh resonator made from a Nb film deposited by sputtering on silicon substrate[16]. Regarding the surface roughness (Such as 0.40 nm for Al/Sapphire and 0.58 nm for Nb/Si) in these references and 1.09 nm for the Ta (110)/Sapphire here, it is fair to infer that Ta_2O_5 layer has a lower

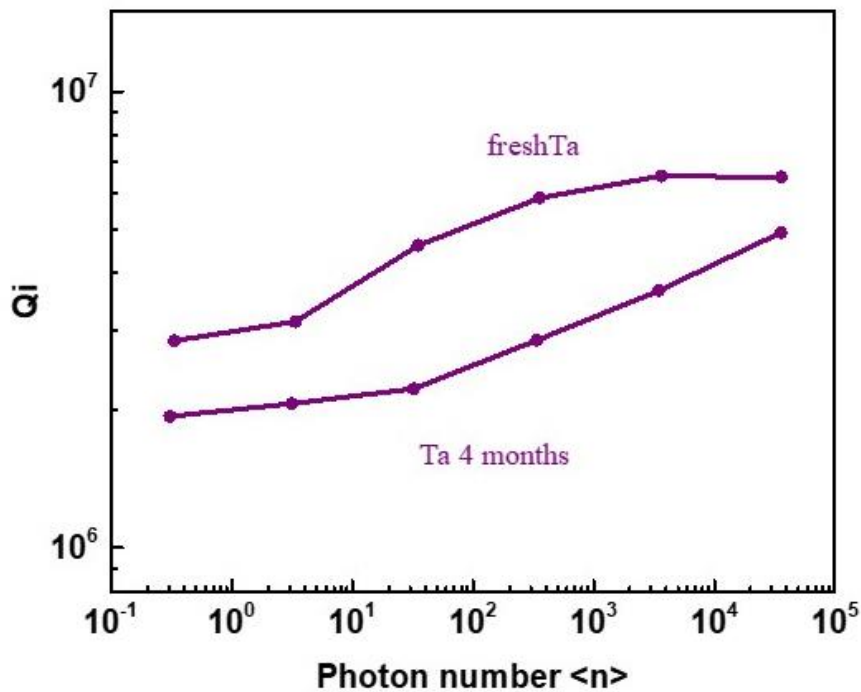


Fig. 3 The power dependence of the Ta film resonator Q_i measured immediately and after 4 months.

dielectric loss than that of the amorphous oxide layer formed in air on Al and Nb film surfaces. For the resonator left in air for four months, a slight degradation is observed.

In view of many factors, like surface contamination, can substantially plague the resonator, the Q_i of 2.0×10^6 is quite remarkable. The robustness of the resonator further implies that the amorphous Ta_2O_5 layer is stable in atmosphere.

To fully make use of the stability and low loss properties of the Ta_2O_5 , an all-tantalum superconducting qubit using the Ta_2O_5 as the dielectric and passivation layer is proposed. Fig. 4 shows the technique to fabricate the Ta/ Ta_2O_5 /Ta Josephson junctions (JJs), and outlines the key fabrication steps for qubits. Before depositing Ta, substrates such as high resistivity silicon or sapphire are pretreated to ensure the clean surface and minimize dielectric loss. Then, a quasi-epitaxial Ta (110) layer with high crystallinity and smooth surface is deposited on the substrate [Fig. 4(b)]. The Ta layer is the bottom electrode of JJs, as well as the foundation of the tunnel barrier layer. Fig. 4(c) gives the Ta_2O_5 tunnel barrier layer. Piranha solution may be applied to oxidize the Ta surface and densify the Ta_2O_5 oxidation layer. Another Ta (110) layer is deposited on Ta_2O_5 layer as the top electrode layer [Fig. 4(d)]. The pattern of JJs is defined using photolithography [Fig. 4(e)], and dry etching process is suggested because of its stable and highly anisotropic characteristic[8]. The etched surface is passivated to protect the whole JJs and other large area structures [Fig. 4(f)]. Piranha solution treatment is recommended because all structure surfaces can be covered by a the amorphous Ta_2O_5 layer. Additionally, piranha solution can remove organic impurities, such as residual photoresist. Then, as shown in Fig. 4(g), large area structures such as resonators and capacitors are patterned into the bottom Ta layer to break the junction from

surroundings. The surfaces are passivated again with piranha solution (Fig. 4(h)). Later, the Ta bridge layer can be deposited between the bottom electrode of JJs and the big structure to form functional circuits (Fig. 4(i)). The process is CMOS compatible and provides scalability for superconducting quantum chips.

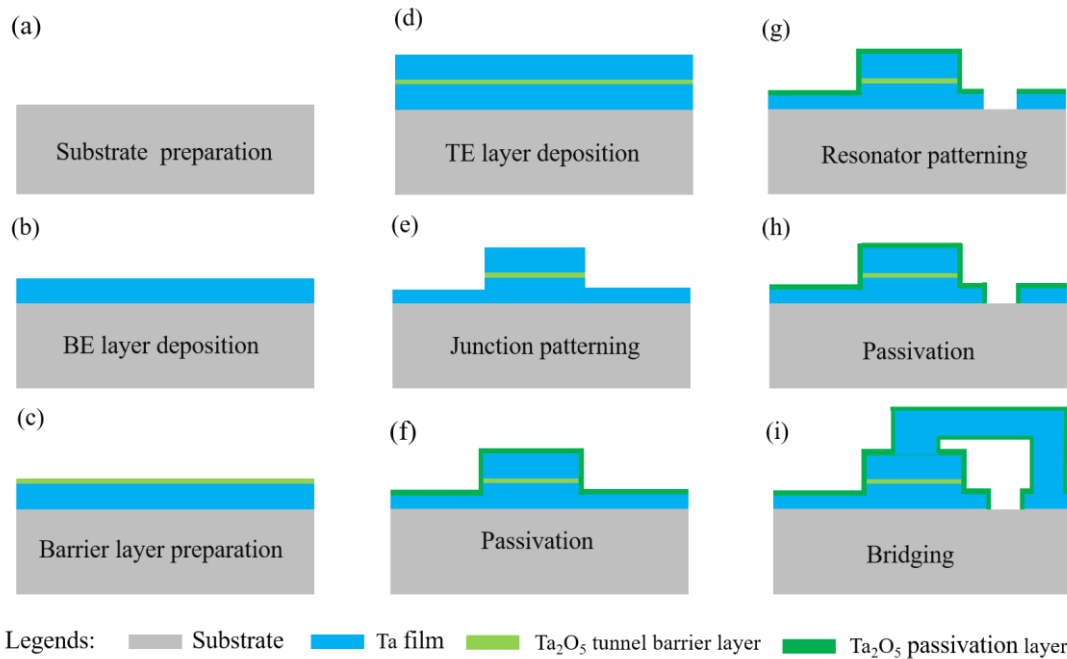


Fig.4 The process flow for the preparation of superconducting qubits based on Ta₂O₅ as dielectric and passivation layers. (a) Preparing the substrate; (b) Depositing Ta film for the bottom electrode (BE) layer of Josephson junctions and other circuit structures; (c) Preparing the Ta₂O₅ tunnel barrier layer for the Josephson junctions; (d) Depositing Ta film for the top electrode (TE) of Josephson junctions; (e) Patterning the junction area; (f) Surface passivation to obtain Ta₂O₅ passivation layer; (g) Patterning the resonators and other circuit structures, (h) Surface passivation to obtain Ta₂O₅ passivation layer; (i) Bridging the TE of the Josephson junctions to the big structures.

4. Conclusion

In conclusion, we have shown that a kind of amorphous Ta₂O₅ is stable in atmosphere and of low dielectric loss. It forms in a self-limiting process on the α -Ta (110) film surface in piranha solution. The thickness and chemical composition of the oxide is robust and uniform. Resonator made from the as deposited α -Ta (110) film on sapphire substrates covered with this kind of Ta₂O₅ layer exhibits high Q_i of 3.0×10^6 in the single photon regime. After exposed to air for months, Q_i of 2.0×10^6 is measured. All-tantalum superconducting qubit using this kind of Ta₂O₅ as the dielectric and passivation layers is proposed, which may provide a new direction for the fabrication and scalability of superconducting quantum chips.

Declaration of Competing Interest

The authors declare no competing interests

Acknowledgements

K. L. X acknowledges support from the Youth Innovation Promotion Association of Chinese Academy of Sciences (2019319). J. G. F. acknowledges support from the Start-up foundation of Suzhou Institute of Nano-Tech and Nano-Bionics, CAS, Suzhou (Y9AAD110).

Data availability statement

The data that support the findings of this study are available from the corresponding author upon reasonable request.

References

- [1] R. Barends, J. Kelly, A. Megrant, A. Veitia, D. Sank, E. Jeffrey, T.C. White, J. Mutus, A.G. Fowler, B. Campbell, Y. Chen, Z. Chen, B. Chiaro, A. Dunsworth, C. Neill, P. O'Malley, P. Roushan, A. Vainsencher, J. Wenner, A.N. Korotkov, A.N. Cleland, J.M. Martinis, Superconducting quantum circuits at the surface code threshold for fault tolerance, *Nature* 508 (2014) 500-503, <https://doi.org/10.1038/nature13171>.
- [2] F. Arute, K. Arya, R. Babbush, D. Bacon, J.C. Bardin, R. Barends, R. Biswas, S. Boixo, F. Brandao, D.A. Buell, B. Burkett, Y. Chen, Z. Chen, B. Chiaro, R. Collins, W. Courtney, A. Dunsworth, E. Farhi, B. Foxen, A. Fowler, C. Gidney, M. Giustina, R. Graff, K. Guerin, S. Habegger, M.P. Harrigan, M.J. Hartmann, A. Ho, M. Hoffmann, T. Huang, T.S. Humble, S.V. Isakov, E. Jeffrey, Z. Jiang, D. Kafri, K. Kechedzhi, J. Kelly, P.V. Klimov, S. Knysh, A. Korotkov, F. Kostritsa, D. Landhuis, M. Lindmark, E. Lucero, D. Lyakh, S. Mandra, J.R. McClean, M. McEwen, A. Megrant, X. Mi, K. Michielsen, M. Mohseni, J. Mutus, O. Naaman, M. Neeley, C. Neill, M.Y. Niu, E. Ostby, A. Petukhov, J.C. Platt, C. Quintana, E.G. Rieffel, P. Roushan, N.C. Rubin, D. Sank, K.J. Satzinger, V. Smelyanskiy, K.J. Sung, M.D. Trevithick, A. Vainsencher, B. Villalonga, T. White, Z.J. Yao, P. Yeh, A. Zalcman, H. Neven, J.M. Martinis, Quantum supremacy using a programmable superconducting processor, *Nature* 574 (2019) 505-510, <https://doi.org/10.1038/s41586-019-1666-5>.
- [3] M.H. Devoret, R.J. Schoelkopf, Superconducting circuits for quantum information:

an outlook, Science 339 (2013) 1169-1174,
<https://doi.org/10.1126/science.1231930>.

- [4] M. Kjaergaard, M.E. Schwartz, J. Braumüller, P. Krantz, J.I.-J. Wang, S. Gustavsson, W.D. Oliver, Superconducting qubits: Current state of play, *Annu. Rev. Condens. Matter Phys.* 11 (2020) 369-395, <https://doi.org/10.1146/annurev-conmatphys-031119-050605>.
- [5] A. Premkumar, C. Weiland, S. Hwang, B. Jäck, A.P.M. Place, I. Waluyo, A. Hunt, V. Bisogni, J. Pellicciari, A. Barbour, M.S. Miller, P. Russo, F. Camino, K. Kisslinger, X. Tong, M.S. Hybertsen, A.A. Houck, I. Jarrige, Microscopic relaxation channels in materials for superconducting qubits, *Commun. Mater.* 2 (2021) 72, <https://doi.org/10.1038/s43246-021-00174-7>.
- [6] I. Siddiqi, Engineering high-coherence superconducting qubits, *Nat. Rev. Mater.* 6 (2021) 875-891, <https://doi.org/10.1038/s41578-021-00370-4>.
- [7] A.P.M. Place, L.V.H. Rodgers, P. Mundada, B.M. Smitham, M. Fitzpatrick, Z. Leng, A. Premkumar, J. Bryon, A. Vrajitoarea, S. Sussman, G. Cheng, T. Madhavan, H.K. Babla, X.H. Le, Y. Gang, B. Jack, A. Gyenis, N. Yao, R.J. Cava, N.P. de Leon, A.A. Houck, New material platform for superconducting transmon qubits with coherence times exceeding 0.3 milliseconds, *Nat. Commun.* 12 (2021) 1779, <https://doi.org/10.1038/s41467-021-22030-5>.
- [8] C. Wang, X. Li, H. Xu, Z. Li, J. Wang, Z. Yang, Z. Mi, X. Liang, T. Su, C. Yang, G. Wang, W. Wang, Y. Li, M. Chen, C. Li, K. Linghu, J. Han, Y. Zhang, Y. Feng,

- Y. Song, T. Ma, J. Zhang, R. Wang, P. Zhao, W. Liu, G. Xue, Y. Jin, H. Yu, Towards practical quantum computers: transmon qubit with a lifetime approaching 0.5 milliseconds, *npj Quantum Information* 8 (2022) 1-6, <https://doi.org/10.1038/s41534-021-00510-2>.
- [9] C.R.H. McRae, H. Wang, J. Gao, M.R. Vissers, T. Brecht, A. Dunsworth, D.P. Pappas, J. Mutus, Materials loss measurements using superconducting microwave resonators, *Rev. Sci. Instrum.* 91 (2020) 091101, <https://doi.org/10.1063/5.0017378>.
- [10] A.A. Murthy, J. Lee, C. Kopas, M.J. Reagor, A.P. McFadden, D.P. Pappas, M. Checchin, A. Grassellino, A. Romanenko, TOF-SIMS analysis of decoherence sources in superconducting qubits, *Appl. Phys. Lett.* 120 (2022) 044002, <https://doi.org/10.1063/5.0079321>.
- [11] K. Xiong, J. Feng, Y. Zheng, J. Cui, M. Yung, S. Zhang, S. Li, H. Yang, Materials in superconducting quantum circuits, *Chin. Sci. Bull.* 67 (2022) 143-162, <https://doi.org/10.1360/TB-2021-0479>.
- [12] C.J.K. Richardson, N.P. Siwak, J. Hackley, Z.K. Keane, J.E. Robinson, B. Arey, I. Arslan, B.S. Palmer, Fabrication artifacts and parallel loss channels in metamorphic epitaxial aluminum superconducting resonators, *Supercond. Sci. Technol.* 29 (2016) 064003, <https://doi.org/10.1088/0953-2048/29/6/064003>.
- [13] A. Megrant, C. Neill, R. Barends, B. Chiaro, Y. Chen, L. Feigl, J. Kelly, E. Lucero, M. Mariantoni, P.J.J. O'Malley, D. Sank, A. Vainsencher, J. Wenner, T.C. White,

- Y. Yin, J. Zhao, C.J. Palmstrøm, J.M. Martinis, A.N. Cleland, Planar superconducting resonators with internal quality factors above one million, *Appl. Phys. Lett.* 100 (2012) 113510, <https://doi.org/10.1063/1.3693409>.
- [14] C.T. Earnest, J.H. Béjanin, T.G. McConkey, E.A. Peters, A. Korinek, H. Yuan, M. Mariantoni, Substrate surface engineering for high-quality silicon/aluminum superconducting resonators, *Supercond. Sci. Technol.* 31 (2018) 125013, <https://doi.org/10.1088/1361-6668/aae548>.
- [15] C.J.K. Richardson, A. Alexander, C.G. Weddle, B. Arey, M. Olszta, Low-loss superconducting titanium nitride grown using plasma-assisted molecular beam epitaxy, *J. Appl. Phys.* 127 (2020) 235302, <https://doi.org/10.1063/5.0008010>.
- [16] J. Verjauw, A. Potočnik, M. Mongillo, R. Acharya, F. Mohiyaddin, G. Simion, A. Pacco, T. Ivanov, D. Wan, A. Vanleenhove, L. Souriau, J. Jussot, A. Thiam, J. Swerts, X. Piao, S. Couet, M. Heyns, B. Govoreanu, I. Radu, Investigation of Microwave Loss Induced by Oxide Regrowth in High-Q Niobium Resonators, *Phys. Rev. Appl.* 16 (2021) 014018, <https://doi.org/10.1103/PhysRevApplied.16.014018>.
- [17] K. Zheng, D. Kowsari, N. Thobaben, X. Du, X. Song, S. Ran, E. Henriksen, D. Wisbey, K. Murch, Nitrogen plasma passivated niobium resonators for superconducting quantum circuits, *Appl. Phys. Lett.* 120 (2022) 102601, <https://doi.org/10.1063/5.0082755>.
- [18] C. Palacio, J. Martinez-Duart, The oxidation of polycrystalline tantalum at low

pressures and low temperatures, *Thin Solid Films* 90 (1982) 63-67,
[https://doi.org/10.1016/0040-6090\(82\)90072-4](https://doi.org/10.1016/0040-6090(82)90072-4).

[19] J. Sanz, S. Hofmann, Auger electron spectroscopy and X-ray photoelectron spectroscopy studies of the oxidation of polycrystalline tantalum and niobium at room temperature and low oxygen pressures, *J. Less-Common Met.* 92 (1983) 317-327, [https://doi.org/10.1016/0022-5088\(83\)90498-8](https://doi.org/10.1016/0022-5088(83)90498-8).

[20] Y. Zhao, H. Gao, R. Huang, Z. Huang, F. Li, J. Feng, Q. Sun, A. Dingsun, H. Yang, Precise determination of surface band bending in Ga-polar n-GaN films by angular dependent X-Ray photoemission spectroscopy, *Sci. Rep.* 9 (2019) 16969, <https://doi.org/10.1038/s41598-019-53236-9>.